AGU PUBLICATIONS

JGR

Journal of Geophysical Research: Solid Earth

RESEARCH ARTICLE
10.1002/2014JB011506

Special Section:
Stress, Strain and Mass Changes at Volcanoes

Gravity changes and deformation at Kīlauea Volcano, Hawaii, associated with summit eruptive activity, 2009–2012

Marco Bagnardi[1,2], Michael P. Poland[3], Daniele Carbone[4], Scott Baker[5], Maurizio Battaglia[6,7], and Falk Amelung[1]

[1]Division of Marine Geology and Geophysics, RSMAS, University of Miami, Coral Gables, Florida, USA, [2]Now at School of Earth and Environment, University of Leeds, Leeds, UK, [3]Hawaiian Volcano Observatory, U.S. Geological Survey, Hawaii, USA, [4]Sezione di Catania, Osservatorio Etneo, Istituto Nazionale di Geofisica e Vulcanologia, Catania, Italy, [5]UNAVCO, Boulder, Colorado, USA, [6]Department of Earth Sciences, Sapienza, University of Rome, Rome, Italy, [7]Volcano Science Center, U.S. Geological Survey, Menlo Park, California, USA

Key Points:
- Mass accumulation at Kilauea Volcano inferred from microgravity measurements
- Magma outgassing at the summit may cause mass increase without uplift
- Rates of gravity increase are correlated with the volcanic activity

Supporting Information:
- Readme
- Figure S1
- Figure S2
- Figure S3
- Figure S4
- Figure S5
- Table S1
- Table S2
- Table S3
- Table S4
- Table S5

Correspondence to:
M. Bagnardi,
M.Bagnardi@leeds.ac.uk

Citation:
Bagnardi, M., M. P. Poland, D. Carbone, S. Baker, M. Battaglia, and F. Amelung (2014), Gravity changes and deformation at Kīlauea Volcano, Hawaii, associated with summit eruptive activity, 2009–2012, *J. Geophys. Res. Solid Earth*, *119*, doi:10.1002/2014JB011506.

Received 30 JUL 2014
Accepted 13 AUG 2014
Accepted article online 19 AUG 2014

Abstract Analysis of microgravity and surface displacement data collected at the summit of Kīlauea Volcano, Hawaii (USA), between December 2009 and November 2012 suggests a net mass accumulation at ~1.5 km depth beneath the northeast margin of Halema'uma'u Crater, within Kīlauea Caldera. Although residual gravity increases and decreases are accompanied by periods of uplift and subsidence of the surface, respectively, the volume change inferred from the modeling of interferometric synthetic aperture radar deformation data can account for only a small portion (as low as 8%) of the mass addition responsible for the gravity increase. We propose that since the opening of a new eruptive vent at the summit of Kīlauea in 2008, magma rising to the surface of the lava lake outgasses, becomes denser, and sinks to deeper levels, replacing less dense gas-rich magma stored in the Halema'uma'u magma reservoir. In fact, a relatively small density increase ($<200\,kg\,m^{-3}$) of a portion of the reservoir can produce the positive residual gravity change measured during the period with the largest mass increase, between March 2011 and November 2012. Other mechanisms may also play a role in the gravity increase without producing significant uplift of the surface, including compressibility of magma, formation of olivine cumulates, and filling of void space by magma. The rate of gravity increase, higher than during previous decades, varies through time and seems to be directly correlated with the volcanic activity occurring at both the summit and the east rift zone of the volcano.

1. Introduction

Microgravity measurements (also referred to as dynamic, campaign, or 4-D gravity) have been collected at Kīlauea Volcano, on the Island of Hawai'i (USA), since 1975 and, when combined with deformation measurements, have yielded important insights into mass change within the volcano [*Dzurisin et al.*, 1980; *Jachens and Eaton*, 1980; *Johnson*, 1992; *Kauahikaua and Miklius*, 2003; *Johnson et al.*, 2010; *Carbone and Poland*, 2012; *Carbone et al.*, 2013]. Campaign gravity and leveling data spanning the 29 November 1975 M_w 7.7 Kalapana earthquake revealed that mass loss beneath the summit due to drainage of magma into Kīlauea's rift zones was larger than expected given the measured surface subsidence, implying the creation of void space [*Dzurisin et al.*, 1980; *Jachens and Eaton*, 1980]. Subsequent surveys, extending through 2008, indicated a steady mass gain (residual gravity increase up to 450 μGal during 1975–2008) accompanied by subsidence (maximum of almost 2 m) near Halema'uma'u Crater within Kīlauea Caldera, which suggests filling of void space by magma [*Johnson et al.*, 2010] or accommodation of additional magma volume by rifting of the summit [*Zurek and Williams-Jones*, 2013]. Since March 2008, a new long-term eruption has been occurring at Kīlauea's summit, and a fissure eruption interrupted the ongoing (since 1983) east rift zone (ERZ) eruption in March 2011 (Figure 1).

We completed five gravity surveys of the Kīlauea summit network between December 2009 and November 2012 to assess whether the gravity increase measured during 1975–2008 continued and also how recent volcanic activity impacted the distribution of mass within the summit reservoir system. The new surveys have a higher temporal resolution (5–15 months) than previous measurements, which were carried out only once every several years. The 2009–2012 time interval includes periods of both summit inflation and deflation, as deduced from interferometric synthetic aperture radar (InSAR) data, and also spans variations in

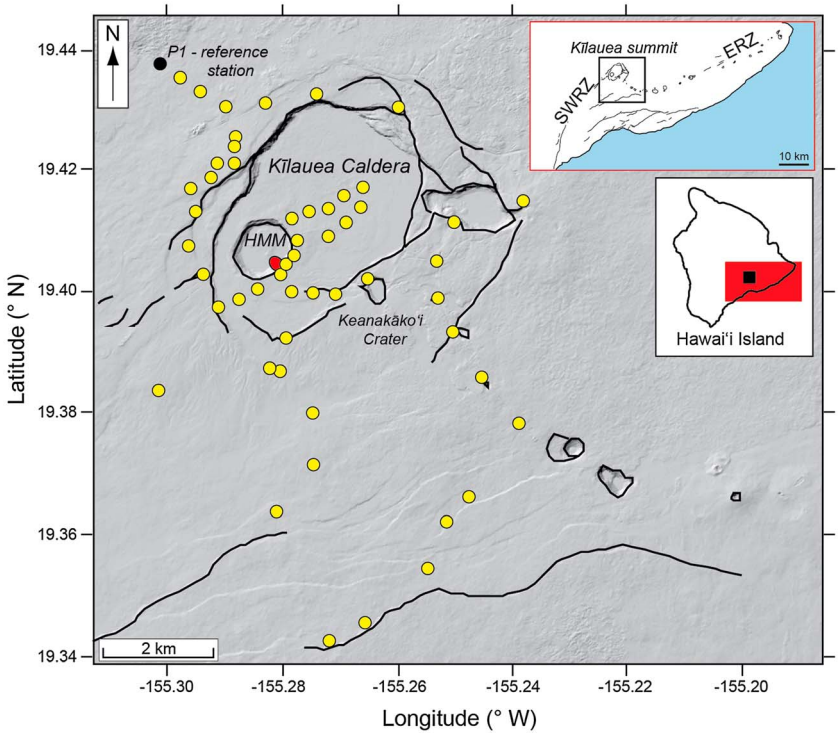

Figure 1. Shaded relief map of the summit of Kīlauea Volcano. Yellow circles indicate the locations of gravity stations that were measured in 2012. The location of the reference station P1 is marked by a black circle. HMM = Halema'uma'u Crater. Red ellipse marks the location of the summit eruptive vent, which hosts an actively circulating lava lake. Black lines outline major faults and craters. Insets show the location of Kīlauea's summit with respect to Hawai'i Island and other features of the volcano. ERZ = east rift zone. SWRZ = southwest rift zone.

summit and ERZ eruptive activity. We modeled the gravity variation and deformation using analytical solutions to infer mass and volume changes over the 3 years spanned by the surveys. Our results indicate that mass continued to accumulate beneath the summit of Kīlauea through November 2012. Although surface uplift was also measured, the increase in reservoir volume inferred from elastic models of surface displacement is an order of magnitude smaller than that needed to produce the measured gravity changes, assuming the volume was filled by basaltic magma. This suggests that the mass increase has occurred through mechanisms that do not produce significant uplift of the surface.

2. Kīlauea Volcano

Kīlauea has been erupting continuously since 1983 from vents on the volcano's ERZ (Figure 1) [*Heliker and Mattox*, 2003]. The first 20 years of the eruption were characterized by ~2 m of subsidence of the south part of the caldera [*Cervelli and Miklius*, 2003; *Johnson et al*., 2010], beneath which lies the volcano's main magma storage area centered at ~2.5–5 km depth [*Eaton*, 1959, 1962; *Dvorak et al*., 1983; *Davis*, 1986; *Delaney et al*., 1990, 1993; *Cervelli and Miklius*, 2003; *Baker and Amelung*, 2012]. The residual gravity change associated with the south caldera source during this time period consisted of a small decrease, suggesting that most of the magma that intruded the volcano was transported to the ERZ and that summit subsidence was a combination of several processes, including extension due to seaward motion of the volcano's south flank [*Johnson*, 1987, 1992; *Kauahikaua and Miklius*, 2003; *Plattner et al*., 2013]. Subsidence switched to uplift during 2003–2007 due to a surge in magma supply to the volcano [*Poland et al*., 2012]. The sources of uplift were not only the south caldera magma reservoir but also small reservoirs ~1–2 km beneath the east margin of Halema'uma'u Crater [*Cervelli and Miklius*, 2003; *Poland et al*., 2009; *Montgomery-Brown et al*., 2010; *Baker and Amelung*, 2012; *Lundgren et al*., 2013] and ~2.5–5 km depth near Keanakāko'i Crater [*Baker and Amelung*, 2012; *Poland et al*., 2012]. Unlike the south caldera source, the shallow Halema'uma'u reservoir experienced a large mass increase during 1975–2008, but the lack of coincident inflation led *Johnson et al*. [2010] to propose that magma

Table 1. Gravity Surveys at Kīlauea's Summit 2009–2012

Date of Survey	Measured Stations	Average Standard Deviation (μGal)
2–18 December 2009	47	13.1
25 June to 16 July 2010	49	12.8
15–25 March 2011	53	11.9
1–22 June 2012	55	14.9
23 October to 28 November 2012	55	12.0

was filling subsurface void space and *Zurek and Williams-Jones* [2013] to speculate that rifting of the summit led to additional magma accumulation without uplift. Summit deformation fluctuated after 2007, with inflation and deflation tied to changes in ERZ eruptive activity [*Poland et al*., 2008, 2012; *Lundgren et al*., 2013].

Coincident with the ongoing ERZ activity, an eruption started at the summit of Kīlauea with the opening of a pit crater along the southeastern margin of Halema'uma'u Crater (HMM in Figure 1) on 19 March 2008 [*Wilson et al*., 2008; *Houghton et al*., 2011; *Orr et al*., 2013]. The new vent is located within a few hundred meters of the positive gravity change measured during 1975–2008. Since its formation, rim and wall collapses have enlarged the opening of the pit from an initial diameter of 35 m to over 220 m by November 2012 [*Richter et al*., 2013; *Orr et al*., 2013]. A lava lake was observed within the vent in September 2008, and since then, the level of its surface has experienced multiple cycles of rise and fall [*Patrick et al*., 2011; *Orr et al*., 2013], reaching a maximum height of 1006 m above sea level (asl) (~22 m beneath the floor of the Halema'uma'u Crater) in October 2012. These cycles follow the general pattern of surface deformation, with the lava lake level rising during periods of summit inflation and falling during deflation—a mechanism that suggests a direct coupling to pressure variations within the plumbing system of the volcano [*Patrick and Orr*, 2011]. The connection between the surface of the lava lake and the areas of magma storage is probably not constant but allowed by a network of cracks that intermittently open and close in response to localized pressure changes [e.g., *Chouet et al*., 2010; *Chouet and Dawson*, 2011]. When pressure increases, these pathways are opened and batches of magma are allowed to rise toward the surface of the lava lake.

Two continuously recording gravimeters were installed in 2010 at the summit of Kīlauea to track gravity change associated with the new eruptive vent; these installations proved excellent at characterizing short-term changes in gravity and eruptive activity. For example, in May–June 2010, the instruments detected a gravity oscillation with a period of 2–5 min that had a source in the shallow Halema'uma'u magma reservoir and may have been related to rapid magma convection [*Carbone and Poland*, 2012]. The gravity signal during draining of the summit lava lake associated with the March 2011 ERZ Kamoamoa fissure eruption [*Lundgren et al*., 2013] was used to derive the density of the upper ~120 m of the lava lake, which was found to be 950 (±300) kg m^{-3} [*Carbone et al*., 2013]. Although measurements from continuously recording spring gravimeters offer excellent temporal resolution to characterize mass movement on the order of minutes to days, they usually do not provide information on longer-term (weeks to years) processes because of instrumental effects [*Carbone et al*., 2003]. The high cost of gravimeters also prevents the deployment of large arrays at single locations, limiting the spatial resolution of continuous gravity measurements. Campaign gravity surveys across a wide network of stations, on the other hand, can help in resolving long-term gravity changes and constraining the spatial distribution of subsurface mass flow, although the temporal resolution is limited by the repeat time of the campaigns [e.g., *Rymer and Brown*, 1986; *Battaglia et al*., 2008; *de Zeeuw-van Dalfsen et al*., 2013].

3. Data

3.1. Microgravity Data

A network of benchmarks across Kīlauea's summit region was reoccupied 5 times between December 2009 and November 2012 (Figure 1; see Table 1 for specific information about each measurement campaign) using, simultaneously, two Scintrex CG-5 gravimeters (CG-578 and CG-579). The two instruments were calibrated against one another by repeated occupations of three calibration lines: Mauna Kea (Hawaii), Mount Hood (Oregon), and Mount Hamilton (California) [*Barnes*, 1968; *Oliver and Barnes*, 1968]. We found that a single scale factor (0.999736 ± 0.000104 for CG-578 and 0.999343 ± 0.000147 for CG-579) can be used to approximate the linear response of each meter [*Valiant*, 1991].

Data were collected following a daily double-looping procedure consisting of three occupations of the reference station (at the start and end of each loop) and two occupations of selected sites (once during each loop). All gravity

measurements are relative to benchmark P1, located 4 km northwest of the caldera center (black circle in Figure 1), away from any known magma pathways where subsurface mass redistribution could have occurred during the time spanned by the gravity surveys. P1 is therefore assumed to be stable, although the area in which it is located did experience surface deformation (<0.02 m of vertical displacement) coincident with summit deflation and inflation that occurred during and after the March 2011 ERZ eruption, respectively. The assumption of stability can still be justified because the measured vertical displacements would have contributed a gravity signal of no more than ±7 μGal—a value within the overall uncertainty of our measurements and 2 orders of magnitude smaller than the maximum gravity change we measured.

We reduced the gravity measurements using the GTOOLS software [*Battaglia et al*., 2012]. The code first adjusts gravity measurements for solid Earth tides, ocean loading, and instrument drift then computes the weighted least squares-adjusted gravity values and their standard deviations. Specifically,

1. Earth tides are estimated using an improved version of *Longman*'s [1959] model that includes the following: (a) the original formulas by *Bartels* [1957, p. 747] for the Moon longitude, (b) updated values for the astronomical constants from *U.S. Naval Observatory* [2011], and (c) the gravimetric factor for an anelastic Earth [*Agnew*, 2007].
2. Ocean loading is computed using the HARDISP code [*Agnew*, 2010] and ocean loading harmonics from the TPXO7.2 ocean tide model [*Bos and Scherneck*, 2012].
3. Instrument drift is corrected using a linear function.

All corrections are performed up to microGal (μGal) precision, in accordance with the specifications of high-resolution surveys. The average standard deviation of all measurements collected during individual surveys varies between 12 and 15 μGal (Table 1).

Residual gravity changes at each station (Δg_r, in μGal) were then calculated for each time interval as $\Delta g_r = \Delta g - 308.6 \times \Delta h$, where Δg is the gravity change in μGal at one station between two surveys, Δh is the vertical displacement in meters at that station during the same interval, and −308.6 μGal/m is the theoretical free-air gradient [*LaFehr*, 1991]. The use of locally measured free-air gradients (−327.3 μGal/m [*Johnson*, 1992] and −330.25 μGal/m [*Kauahikaua and Miklius*, 2003]) would have not significantly influenced the calculated residual gravity changes during any time interval (maximum discrepancy < 4 μGal at the station with the largest vertical displacement). The vertical displacement was calculated by combining ascending and descending InSAR measurements (see section 3.2) that span the same time interval as the gravity measurements. Although variations in the height of the water table can produce changes in the measured gravity [e.g., *Battaglia and Hill*, 2009], at Kīlauea the water table is ~500 m beneath the surface [*Kauahikaua*, 1993] and experiences only minor fluctuations (J. Kauahikaua, personal communication, 2010). We therefore follow the approach of previous studies [*Johnson*, 1992; *Kauahikaua and Miklius*, 2003; *Johnson et al*., 2010] and do not consider water table effects to be a significant source of gravity change [*Battaglia et al*., 2003b].

3.2. InSAR Data

We used synthetic aperture radar (SAR) data acquired along both ascending and descending orbital passes by the German Space Agency (Deutsches Zentrum für Luft- und Raumfahrt (DLR)) TerraSAR-X satellite (from December 2009 to June 2012) and the Italian Space Agency (Agenzia Spaziale Italiana (ASI)) Cosmo-SkyMed satellite constellation (from June to November 2012). The TerraSAR-X data set includes 74 images from track 24 (descending, beam mode strip_007, incidence angle 31°) and 80 images from track 32 (ascending, beam mode strip_008, incidence angle 33°). The Cosmo-SkyMed data set is composed of 10 images from an ascending track (incidence angle 39°) and 12 images from a descending track (incidence angle 41°).

The TerraSAR-X interferograms were processed using the Jet Propulsion Laboratory/Caltech ROI_PAC SAR Software [*Rosen et al*., 2004], while the Cosmo-SkyMed data were processed using the GMTSAR InSAR processing system [*Sandwell et al*., 2011]. We removed the topographic contribution to the interferometric phase using a 30 m resolution digital elevation model generated by the NASA Shuttle Radar Topography Mission [*Farr et al*., 2007]. The interferograms were then phase unwrapped using the statistical-cost, network-flow algorithm for phase unwrapping algorithm [*Chen and Zebker*, 2001].

To resolve the temporal evolution of surface deformation, we used the small-baseline subset method [*Berardino et al*., 2002; *Lanari et al*., 2004; *Fattahi and Amelung*, 2013] and generated InSAR time series with

inversions done independently for each orbital track. InSAR displacement time series are measured along the radar line of sight (LOS), but measurements of the vertical component of the deformation at the time of each gravity survey are necessary to correct the microgravity data for the free-air effect. We therefore combined the InSAR time series results from ascending and descending orbital passes to calculate the vertical component of motion following the method of *Wright et al*. [2004] (for a detailed description of the approach see *Baker and Amelung* [2012] and *Baker* [2012]).

4. Residual Gravity Changes and Deformation at Kīlauea's Summit

Time series of residual gravity changes and vertical deformation during 2009–2012 for selected stations representative of key areas of Kīlauea's summit are presented in Figure 2. The maximum change throughout the entire time interval occurred at station HOVL-G (Figure 2a), which is located 20 m SE of the rim of Halema'uma'u Crater, 80 m above the crater floor, and 150 m east of the center of the summit eruptive vent. This station, which was first measured in July 2010 after installation of a continuously recording gravimeter at the site [*Carbone and Poland*, 2012; *Carbone et al*., 2013], shows a moderate negative change (-39 ± 9 μGal) by the time of its second occupation in March 2011, after the summit of the volcano had subsided in response to an ERZ fissure eruption during 5–9 March 2011 [*Lundgren et al*., 2013]. From March 2011 through November 2012, however, a large positive change of 370 ± 35 μGal is measured at the site during a period of modest uplift (~0.15 m). Two other stations located within 250 m of HOVL-G—HVO41 and 205YY (Figure 2a)—show the same trend in residual gravity, but despite their close proximity, the magnitude of the March 2011 to November 2012 change is lower (226 and 231 μGal at HVO41 and 205YY, respectively).

Significant changes in residual gravity are also observed in the central portion of Kīlauea Caldera (Figure 2b). Stations in this region show similar trends to those located closer to the rim of Halema'uma'u Crater, but gravity changes are smaller in magnitude during March 2011 to November 2012 (80–123 μGal) despite similar ground uplift. Residual gravity changes and deformation at stations located in other areas of Kīlauea's summit, including those over other important features of the volcano's magma plumbing system such as the south caldera (Figure 2c) and the upper ERZ (Figure 2d), are within the uncertainty of the measurements and indicate no significant change in subsurface mass.

To better resolve the spatial characteristics of changes in gravity and deformation, we divided the 3 year time interval (December 2009 to November 2012) into four periods defined by the epochs of the gravity surveys. For all periods, we present the residual gravity changes measured at each station together with their uncertainty (1 standard deviation, Figure 3) and the surface displacement in the LOS direction measured by InSAR time series (Figure 4).

During the first time period, between December 2009 and July 2010, a positive residual gravity anomaly is centered on and limited to the summit caldera (Figure 3a). The magnitude of this anomaly is moderate (53 ± 20 μGal at its maximum), but its spatial distribution matches the area of uplift also centered on the summit caldera, which is visible in the InSAR-derived surface displacement map (Figure 4a). This same period is characterized by broad subsidence south of the caldera and along the southwest rift zone (SWRZ) of the volcano, but stations located in these areas do not show any consistent residual gravity change.

The second period, starting in July 2010 and ending 2 weeks after the end of the March 2011 ERZ fissure eruption, is not characterized by large gravity changes, although negative values are present across the summit (Figure 3b). A few outliers are also present but, given their large discrepancy with measurements at nearby stations, can be disregarded. Subsidence of the ground (net maximum deformation −0.06 m) is centered east of Halema'uma'u Crater and merges with the broader subsiding area encompassing the south caldera and the SWRZ (Figure 4b). The net deformation during this period, however, does not reflect the complexity of the changes that took place. During the 5–9 March 2011, ERZ fissure eruption, the area east of Halema'uma'u Crater subsided by a maximum of 0.15 m [*Lundgren et al*., 2013]. Rapid uplift preceded and followed the eruption, reducing the magnitude of the net ground displacement measured between the epochs of the two gravity surveys.

The third and the fourth periods, from March 2011 to June 2012 and from June to November 2012, share similar characteristics to one another. During both time intervals, residual gravity changes are mostly positive, and maximum values occur along the southeast rim of Halema'uma'u Crater (Figures 3c and 3d), with positive

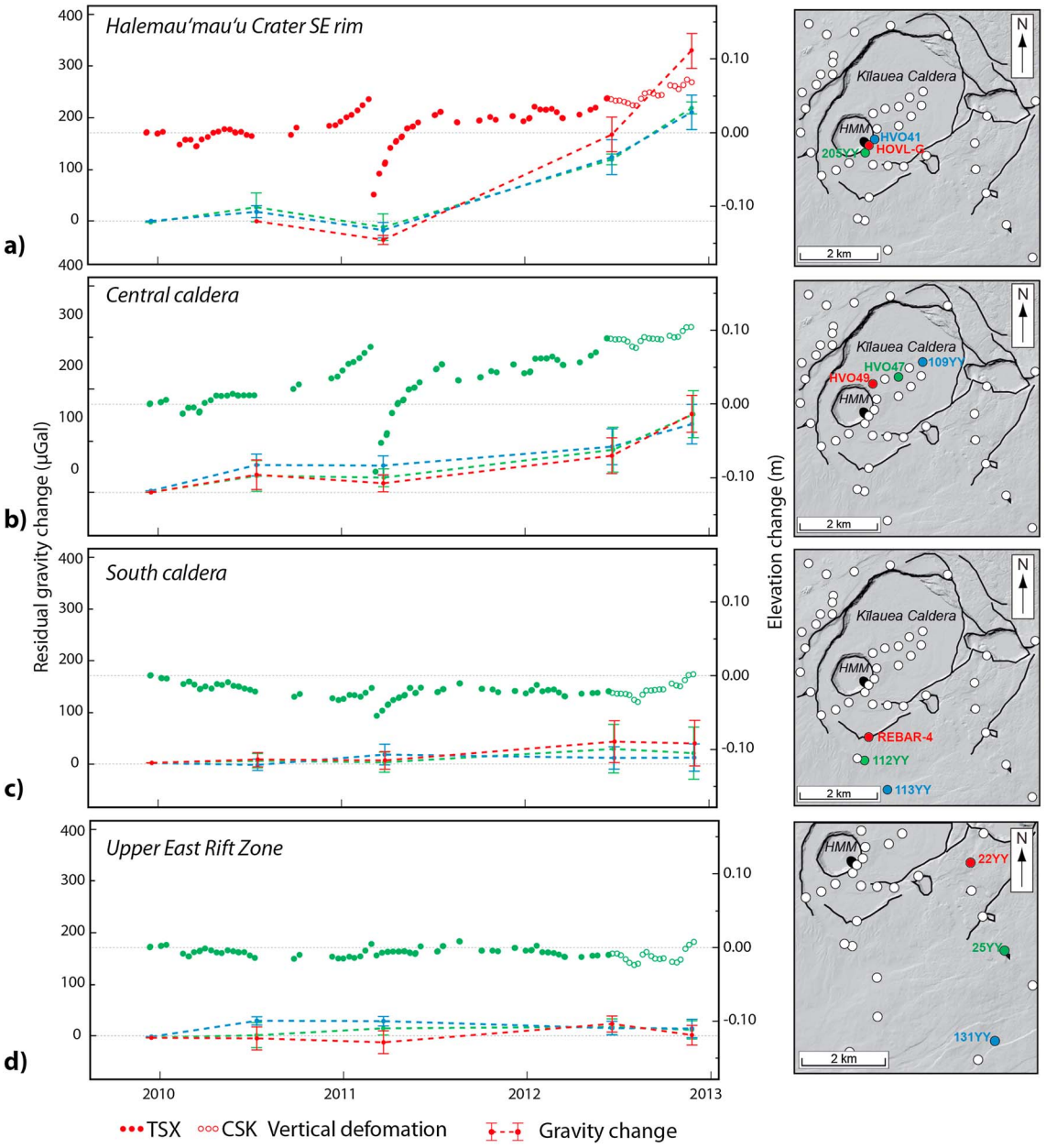

Figure 2. Residual gravity change (error bars) and vertical deformation (filled circles, TSX = TerraSAR-X; open circles, CSK = Cosmo-SkyMed) for selected areas around Kīlauea's summit. (a) Sites located near the SE rim of Halema'uma'u Crater (adjacent to the summit eruptive vent), which show the maximum residual gravity changes over the course of the measurements. (b) Sites located in the central part of the summit caldera. (c) Sites located in the south part of the summit caldera. (d) Sites located in the upper part of the east rift zone. Maps show the location of each station (plot colors correspond to station colors on associated maps). Error bars indicate 1 standard deviation of uncertainty for the residual gravity measurements. Vertical deformation and residual gravity change scales are the same in all plots to highlight differences in the magnitudes of changes between areas. Vertical deformation is obtained from InSAR data (combined LOS displacements from ascending and descending orbits) and is shown at the times of all SAR images acquired during the studied time interval.

changes extending outward from the center of the caldera. Further minor positive changes are present northeast of the caldera during the third period, but when summed with variations measured during the fourth period, they become negligible. Also, these stations do not overlie any known portion of the plumbing system of the volcano, and since they were all measured during the same day of the June 2012 campaign, we believe that these anomalous readings have been possibly caused by systematic errors. InSAR data for both time periods indicate uplift of the caldera centered east of Halema'uma'u Crater, in the same location as the center of subsidence during period 2 (Figures 4c and 4d). Most of the caldera uplift occurs during the months

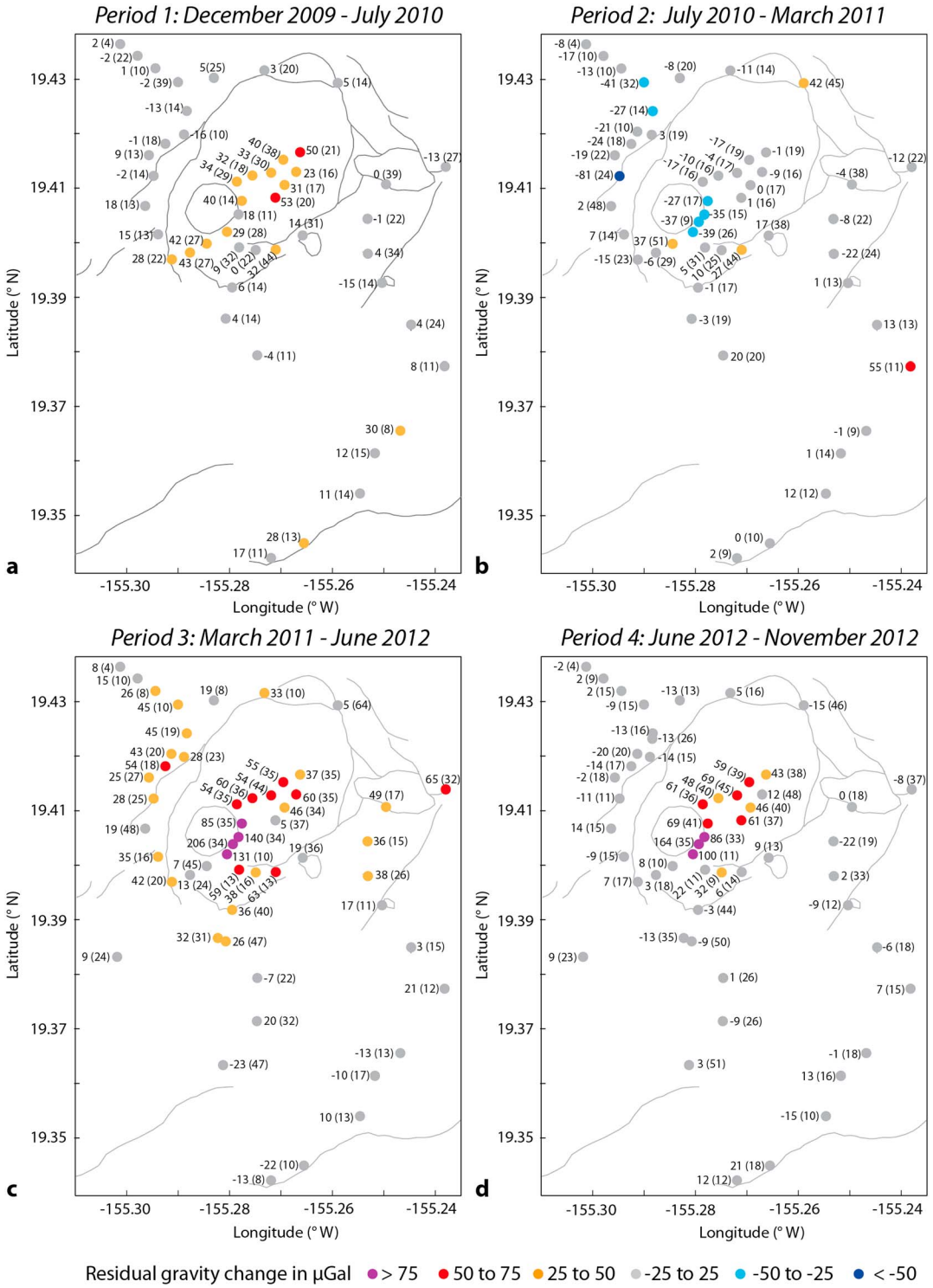

Figure 3. Maps of residual gravity change at Kīlauea's summit. The entire time interval is divided into (a–d) four periods (1 to 4) based on the dates of the gravity surveys. Each station is marked with a filled circle that is color coded according to the magnitude of the gravity change (warm colors indicate positive changes and cold colors indicate negative changes). For each station, the calculated residual gravity change and, in parenthesis, 1 standard deviation of uncertainty are also indicated. Gray lines outline major faults and craters.

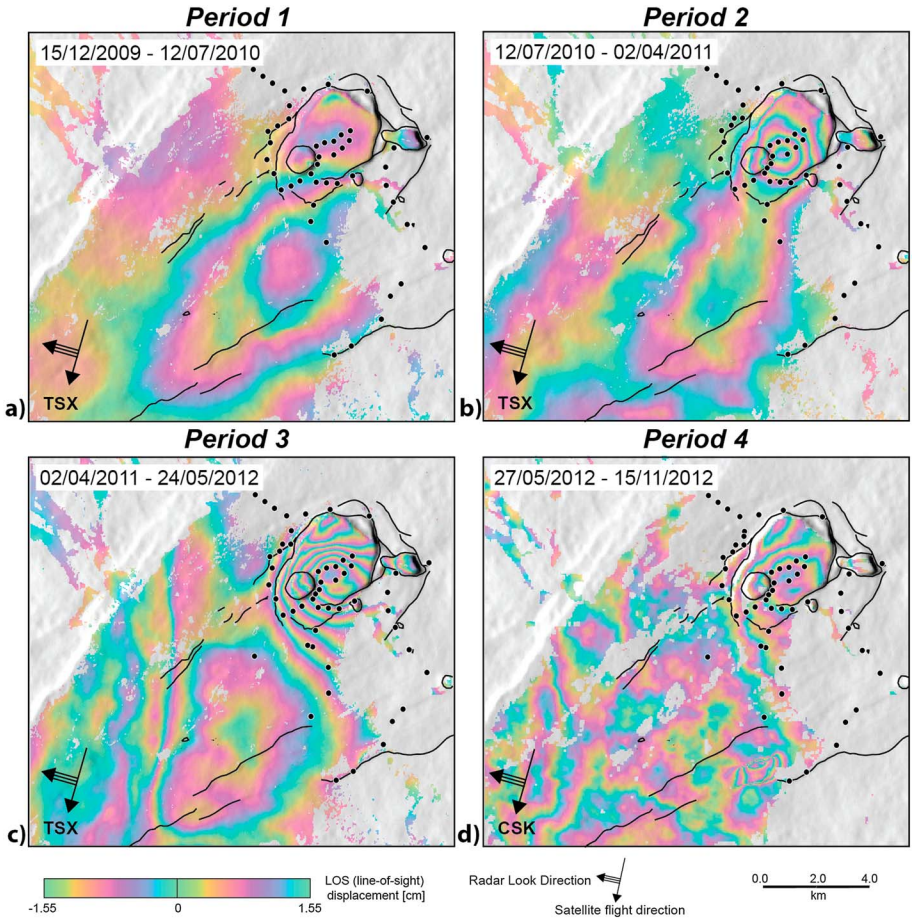

Figure 4. Surface deformation at Kīlauea's summit measured by InSAR time series. The entire time interval is divided into (a–d) four periods (1 to 4) based on the dates of the SAR acquisitions closest to those of the gravity surveys (dates given in upper left of each image). Black circles mark locations of gravity stations, and black lines outline major faults and craters. Satellite flight direction, look direction, and name (TSX = TerraSAR-X; CSK = Cosmo-SkyMed) are reported in each panel. Each fringe (full color cycle) represents 1.55 cm of LOS displacement (positive for uplift, negative for subsidence). Images show mean line-of-sight deformation for each time interval as deduced from time series analysis. (a) Subsidence is centered on the south caldera and upper SWRZ, while uplift is centered near Halema'uma'u Crater. (b) Subsidence characterizes both areas and is at a maximum east of Halema'uma'u Crater. (c) Subsidence is centered on the upper SWRZ, and uplift is centered east of Halema'uma'u Crater. (d) Uplift is centered near Halema'uma'u Crater. In the southern portion of the image, localized deformation is apparent due to normal faulting during an earthquake swarm (max magnitude $M = 3.7$) that occurred in the Koa'e fault zone on 4–5 June 2012.

immediately following the March 2011 ERZ eruption. As during the previous time periods, subsidence characterizes the area south of the caldera and along the SWRZ, but no significant residual gravity changes are measured in these areas.

5. Lava Lake Effect

Continuous gravity measurements have shown that significant gravity changes (tens of microGal) are associated with fluctuations in the level of the lava lake within Kīlauea's summit eruptive vent [*Carbone et al.*, 2013]. Data recorded at the rim of Halema'uma'u Crater during the 14 h long and 120 m drainage of the lava lake, which occurred on 5 March 2011 coincident with the opening of a fissure on the ERZ, showed a gravity decrease of more than 100 μGal. This change was modeled as due to a mass removal from the pit of 2.5×10^6 m^3 of low-density gas-rich magma (<1000 kg m^{-3}). These results indicate that variations in the lava lake level can also influence campaign measurements carried out in the vicinity of the summit eruptive vent. In fact, the maximum residual gravity changes (both positive and negative) calculated from campaign data are in most cases measured at the stations closest to the summit eruptive vent, and values decrease rapidly with distance from the vent.

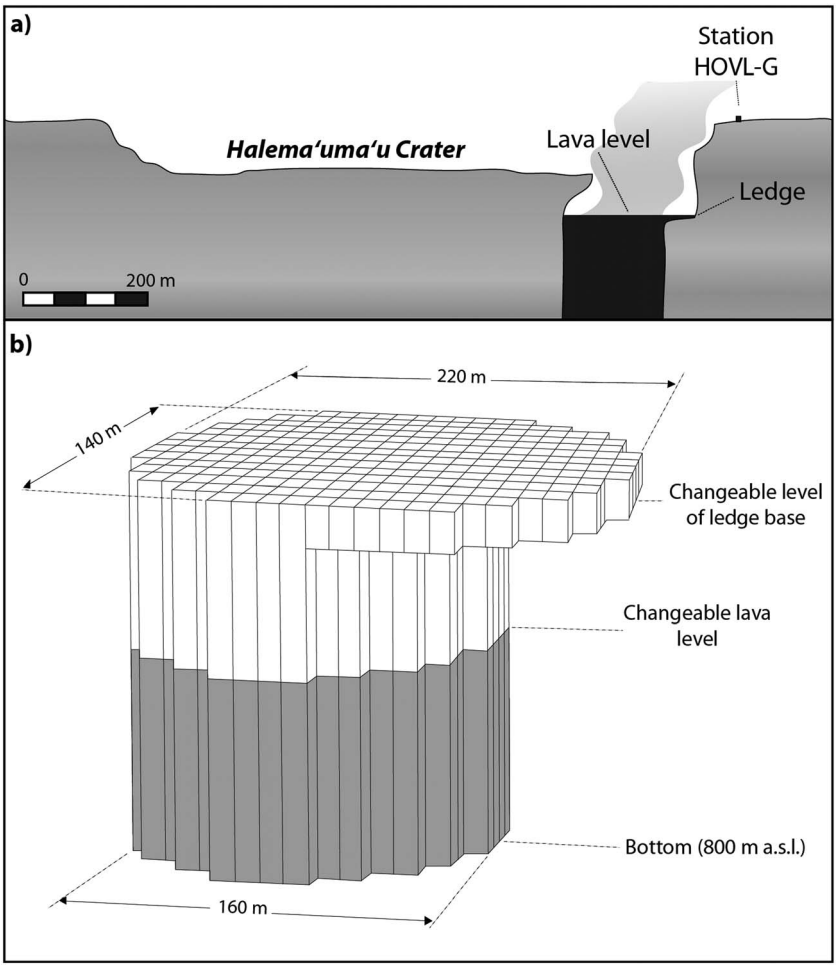

Figure 5. Geometry of summit eruptive vent and model of lava lake, taken from *Carbone et al.* [2013]. (a) Schematic cross section (redrawn from *Orr et al.* [2013]) through Halema'uma'u Crater and the summit eruptive vent and showing vent shape as deduced from visual and lidar observations. (b) Model geometry consisting of 252 vertical square-based (10×10 m) parallelepipeds with changeable height to simulate varying lava levels. The shape of the model is intended to reproduce the asymmetric shape of the eruptive vent.

We assessed the contribution of changes in lava lake level to campaign gravity data using a numerical model that takes into account the pit geometry and the lava height inside the pit at the time of each gravity survey [*Carbone et al.*, 2013]. The geometry of the conduit and of the lava lake surface is inferred from visual observations and ground-based lidar data. While the pit opening at the surface has progressively enlarged through episodic rim and vent wall collapses [*Orr et al.*, 2013; *Richter et al.*, 2013], no significant variations have been observed in the geometry of the vent at the level of the lava lake since the start of our campaign gravity data in December 2009. We therefore assume a constant model geometry for the summit vent for the entire time interval of our gravity measurements.

Our model for the gravity changes due to lava-level variations is the same as *Carbone et al.* [2013]. The pit hosting the lava lake is approximated by a cylinder with an elliptical section that abruptly widens at the top (Figure 5). The bottom is located at 800 m asl (228 m below the floor of Halema'uma'u Crater, which is lower than the minimum height reached by the lava lake during the time of our study) and has a 160 m long major axis oriented NW-SE and a 140 m long minor axis oriented SW-NE. The top portion, forming a "ledge" that is only occasionally flooded by magma, has a major axis of 220 m and the same minor axis as the bottom part. The entire pit is discretized into 252 vertical square-based (10×10 m) parallelepipeds with changeable height. The height of the elements represents the lava level within the pit at a specific time (Table 2) for which we assume a density of 1000 kg m^{-3} [*Carbone et al.*, 2013]. The gravity effect produced by each parallelepiped is calculated [*Talwani*, 1973],

Table 2. Lava Lake Height During the Time of Each Gravity Survey (Min–Max)

Date of Survey	Height asl (m)	Height Below the Floor of Halema'uma'u Crater (m)
December 2009	835	193
June–July 2010	829–854	199–174
March 2011	827–840	201–188
June 2012	936–971	92–57
October–November 2012	949–994	79–34

and the total effect is obtained by summing the contribution of each element. Since we are interested in the lava lake contribution to the measured residual gravity changes, its effect is calculated at the distance of each measurement site and subtracted from the measured gravity changes between surveys.

The calculated lava lake effect is negligible at all campaign gravity stations for the first two time periods (December 2009 to June–July 2010 and June–July 2010 to March 2011) because the lava-level variations between the epochs of the gravity surveys are less than 20 m (resulting in less than 10 μGal of gravity change at the closest stations). For the two subsequent time periods (March 2011 to June 2012 and June 2012 to October–November 2012), however, the lava level is much higher and the level changes are much more significant—the lava lake level rose by up to 167 m between March 2011 and November 2012. In Figure 6a, we show the gravity changes induced by variations in lava lake level calculated for selected stations on the caldera floor. The maximum effect is at HOVL-G, and the effect decreases rapidly with radial distance from the summit vent, becoming almost zero at station HVO48, ~1000 m from the center of the lava lake.

We apply the calculated adjustment to the residual gravity changes at all those stations that are influenced by the lava lake level change contribution (>3 μGal), obtaining new data sets for periods 3 and 4 (Figures 6b and 6c). After this adjustment, the residual values at stations near the rim of Halema'mau'u Crater are similar to those measured in the central portion of the summit caldera (64–86 μGal during period 3 and 65–68 μGal during period 4).

6. Deformation and Gravity Change Modeling

Modeling of deformation and residual gravity was carried out in four steps. First, we performed a nonlinear inversion of the measured LOS displacements, from ascending and descending orbital tracks (spanning approximately the same time intervals), to infer the characteristics of deformation sources that were active between December 2009 and November 2012. These models were then used to track subsurface volume change during each time period spanned by gravity measurements. Successively, we inverted the residual gravity data sets to infer the source of mass change responsible for the observed residual gravity variations. Finally, we compared source depths, locations, and volume/mass changes obtained from the deformation and gravity data.

6.1. Deformation Modeling

Two sources of deformation were active beneath Kīlauea's summit during the 2009–2012 time interval: one caused displacement of the ground just east of Halema'uma'u Crater (hereafter, HMM source) and the second produced broad subsidence along the SWRZ (hereafter, SWRZ source). To constrain these sources, we inverted InSAR data that span time periods when only an individual source is active (Table 3). This approach can reduce the ambiguity caused by modeling two or more overlapping sources of deformation. Also, while the SWRZ source seems to only be associated with subsidence, the HMM source produced both uplift and subsidence. To confirm that both types of deformation are generated by the same source, we inverted for data spanning intervals of both ground uplift and subsidence and then compared the results.

Both sources have been identified and characterized by previous studies [e.g., *Poland et al*., 2012; *Baker and Amelung*, 2012]. We therefore adopted the same approach and used the analytical solution for a finite spherical magma body [*McTigue*, 1987] to model the HMM source and that for a rectangular dislocation source with uniform opening [*Okada*, 1985] to reproduce ground displacement in the SWRZ. Both solutions are for sources embedded in a flat, isotropic, homogeneous, elastic half space (Poisson's ratio $\nu = 0.25$). In the case of the finite spherical magma body we only constrained the source depth, the surface projection of its center, and the changes in volume (ΔV). Although the analytical formulation of this model implies that $\Delta V = (\Delta P \times r^3)/\mu$ [*McTigue*, 1987], where ΔP is the pressure change within the sphere, r the source radius, and μ the shear modulus of the elastic half space, these parameters are not independent from each other (for example, a

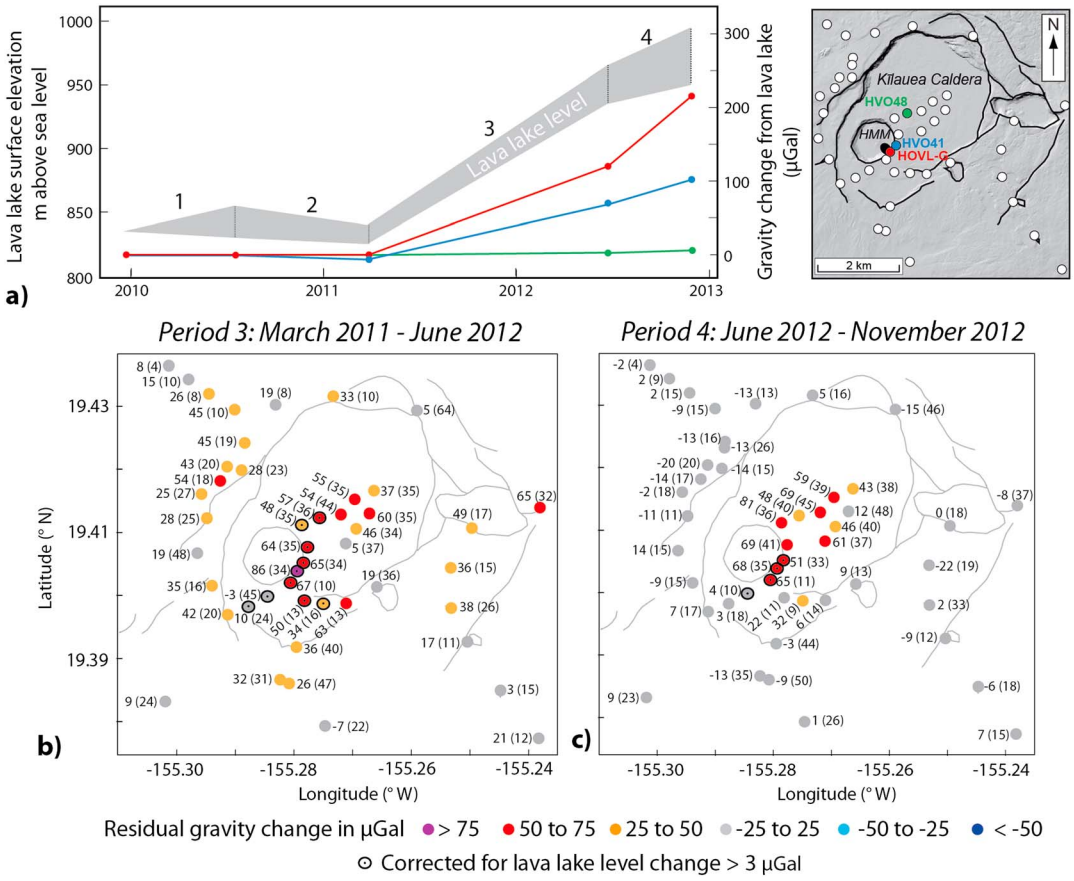

Figure 6. (a) Residual gravity change due to fluctuations in lava lake level. Map shows the location of each station (plot colors correspond to station colors on map). In gray, the elevation of the lava lake surface between gravity surveys is given. Dashed lines indicate the spread in lake height during the course of the surveys (each of which lasted 2–4 weeks). The effect is significant only during periods 3 and 4, and it is a maximum at station HOVL-G. Maps of residual gravity change during (b) period 3 and (c) period 4, after adjustment for the lava lake effect. Each station is marked with a filled circle, which is color coded based on the magnitude of the gravity change (warm colors indicate positive changes, cold colors indicate negative changes). Stations for which the computed adjustment is > 3 μGal are highlighted with a black circle and dot. For each station, the adjusted residual gravity change and, in parenthesis, 1 standard deviation of uncertainty are also indicated. Gray lines outline major faults and craters.

large source radius would correspond to a small pressure change, and vice versa) and, therefore, they cannot be uniquely determined [e.g., *Battaglia et al.*, 2003a; *Battaglia and Hill*, 2009].

Since each original data set consists of ~2.5×10^5 data points, we performed spatial averaging using the *Quadtree* algorithm [*Jonsson et al.*, 2002] to generate the data vectors used in the inversions. The optimal solutions and their probability density distributions were then estimated using the Monte Carlo-based Gibbs sampling (GS) algorithm [*Brooks and Frazer*, 2005]. The quality of the fit of the predicted deformation to the measured displacement was assessed using the normalized root-mean-square error between observed and modeled InSAR LOS displacements.

Table 3. Dates Spanned by Interferograms Used to Characterize the Individual Sources of Deformation

Deformation Source	Satellite	Date 1-Date 2 (Satellite Pass)
South caldera-SWRZ	TerraSAR-X	15/12/2009-12/7/2010 (descending) 16/12/2009-2/7/2010 (ascending)
HMM deflation	TerraSAR-X	17/2/2011-2/4/2011 (descending) 1/3/2011-3/4/2011 (ascending)
HMM inflation	TerraSAR-X	24/4/2011-21/7/2011 (descending) 25/4/2001-22/7/2011 (ascending)

LOS displacements measured during December 2009 to July 2010 (Table 3) were used to constrain the SWRZ source, since deformation within the caldera was minimal. The best fitting model is an ~10.8×0.9 km rectangular source oriented NE-SW and centered at ~3.9 km depth beneath the upper SWRZ (see supporting information). This

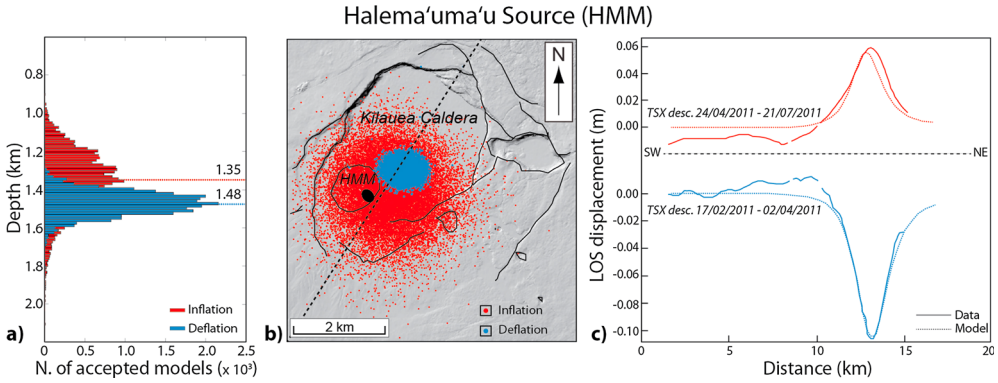

Figure 7. Deformation modeling results for the Halema'uma'u source (HMM). (a) Normalized posterior probability distributions for the depth parameter obtained using the Gibbs sampling algorithm (25,000 samples). In red are the results for a period of inflation and in blue for a period of deflation. Dotted lines represent the depth of the best fitting models. (b) Two-dimensional scatterplot of the latitude and longitude positions for the source of inflation (red) and deflation (blue). (c) Profiles showing the fit of each model (dotted lines) to the data (solid lines). Profile location is given by the black dashed line in Figure 7b.

geometry approximates a contracting sill, although processes other than magma withdrawal may contribute to, or be the predominant cause of, the observed subsidence (e.g., extension due to seaward motion of the volcano's south flank [e.g., *Plattner et al.*, 2013]). The lack of gravity change in this area means that our model assumption of a contracting sill will not influence our interpretations of gravity change in the caldera. It is, however, necessary to account for the superposition of the broad subsidence with the deformation measured inside the caldera which, if not accounted for, will lead to biased estimates of the volume changes for the HMM source.

Surface deformation measured by InSAR data spanning the March 2011 ERZ eruption was used to characterize the HMM source during periods of subsidence, while data spanning the posteruptive summit reinflation, from April to July 2011, provided a means of characterizing the same source during periods of uplift (Table 3). Source depth (Figure 7a) and location (Figure 7b) are best characterized by the deflationary data because of the larger displacement (Figure 7c), but both inversions provide similar results: a spherical source located at ~1.5 km depth (1.2–1.7 km, 95% confidence interval) and centered just east of Halema'uma'u Crater, beneath the area of maximum surface displacement (for detailed results see supporting information). The overlapping results suggest that the same source is responsible for both subsidence and uplift of Kīlauea's summit caldera during the time interval spanned by our gravity surveys. Our results are also very similar to those of an independent study that modeled the summit deflation measured by InSAR (Cosmo-SkyMed satellite) and GPS during the March 2011 ERZ eruption [*Lundgren et al.*, 2013].

The geometries of the SWRZ and HMM sources were then fixed based on the best fits obtained above. Using these parameters, the volume changes during each time period were estimated through nonlinear inversion of the InSAR data (Table 4; see supporting information for further details). Minor volume fluctuations are inferred for the HMM source during periods 1 and 2, while a cumulative volume increase of $1.71 \times 10^6\,m^3$ is obtained from the inversion of deformation data spanning periods 3 and 4.

6.2. Modeling Residual Gravity Changes

Residual gravity changes can be inverted to constrain their source location and associated mass variation. The gravitational attraction of a spherical body of finite size and mass, where mass $m = \rho\,\Delta V$ with ρ as the density of the mass and ΔV the change in volume, is identical to that of a point source with the same mass m:

$$\Delta g_r = G\ m\ \left(d/\left(r^2+d^2\right)^{3/2}\right) \quad (1)$$

where $G = 6.67 \times 10^{-11}\,N\,m^2\,kg^{-2}$ is the universal gravity constant, d is depth of the point source, and r the radial distance from the surface projection of the source [*Battaglia*

Table 4. Volume Changes During Each Time Period[a]

Period	HMM Source ΔV in $\times 10^6\,m^3$
1	0.16 [0.01–0.37]
2	−0.33 [−0.26 to −0.40]
3	1.06 [1.00–1.11]
4	0.65 [0.54–0.77]
Total	1.54 [1.29–1.85]
3 + 4	1.71 [1.54 1.88]

[a]The 95% confidence intervals are shown in brackets.

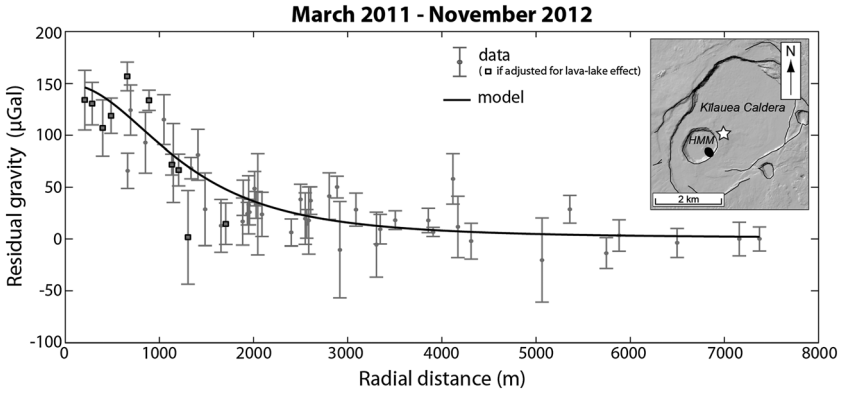

Figure 8. Residual gravity change modeling results. The solid black line gives best fit to residual gravity change recorded between March 2011 and November 2012 (gray error bars). Black squares indicate residual gravity values adjusted for the lava lake effect. The best fitting source is centered at 1.59 km depth beneath the NE margin of Halema'uma'u Crater (white star in the inset) and has a mass addition of 0.56×10^{11} kg. The R^2 value is 0.89.

and Hill, 2009]. The best fit to the measured gravity changes was calculated using MATLAB's built-in *fminsearch* function (*Nelder-Mead* method), which performs an unconstrained nonlinear minimization of the sum of squared residuals (SSR) with respect to the various parameters. The nonlinear minimization requires starting estimates for the fit parameters. To avoid convergence on local minima, we tested 128 random realizations of the initial parameters [*Bergstra and Bengio*, 2012] and used the solution providing the smallest value for the SSR. The goodness of the fit is provided by the value of the coefficient of determination R^2: if $R^2 = 1$, the model is able to explain all variations in the observed data; if $R^2 = 0$, the model is not able to explain any of the observed data. A bootstrap percentile method computed the 95% confidence limits [*Efron and Tibshirani*, 1993].

Gravity changes during periods 1 and 2 are too small compared to the background noise to estimate any significant mass change. Larger variations, on the other hand, characterize periods 3 and 4. Given the similarities in the spatial distribution of the residual gravity changes during these two periods (Figures 6b and 6c), we inverted for the total variations measured between March 2011 and November 2012 (period 3 + period 4). This approach allows us to maximize the signal-to-noise ratio as well. The best fitting source is a point source centered just east of Halema'uma'u Crater (Figure 8)—approximately the same location as the HMM deformation source. The inferred depth of the gravity source, very similar to that of the HMM source of deformation, is 1.59 km (1.35–1.96, 95% confidence interval), and the mass addition is modeled as 0.56×10^{11} kg ($0.45–0.71 \times 10^{11}$ kg, 95% confidence interval). Assuming a density for basaltic magma of $\rho = 2500\ \mathrm{kg\ m^{-3}}$, the associated volume change ΔV would be $22.4 \times 10^6\ \mathrm{m^3}$ ($18.0–28.4 \times 10^6\ \mathrm{m^3}$, 95% confidence interval), which is an order of magnitude larger than the volume change inferred from the deformation data during the same time interval ($1.71 \times 10^6\ \mathrm{m^3}$).

7. Discussion

Significant residual gravity changes (10–10^2 μGal) were measured between December 2009 and November 2012 at the summit of Kīlauea. When adjusted for the effect of variations in lava lake level, these changes indicate a significant mass increase in the shallow magma reservoir beneath the northeast margin of Halema'uma'u Crater. InSAR data spanning the same time interval indicate moderate surface displacements (both uplift and subsidence, <0.20 m) accompanying the gravity changes, also centered northeast of the Halema'uma'u Crater. This location is similar to the loci of gravity increase measured between 1975 and 2008 that was interpreted as the result of magma accumulation in a void space at ~1 km depth [*Johnson et al.*, 2010] or within a volume created by the rifting of the summit [*Zurek and Williams-Jones*, 2013].

Also, as in 1975–2008, during 2009–2012 there were no significant gravity changes south of the caldera, implying no resolvable mass change in the south caldera reservoir. Surface displacement in this area is likewise minor. Subsidence measured in the upper part of the SWRZ during 2009–2012 is not associated with

any significant change in residual gravity (although we must keep in mind that this could be a reflection of the poor distribution of gravity stations in this area), suggesting that the process causing the deformation is not related to subsurface mass flow.

7.1. Rapid Mass Increase

Although residual gravity changes during 2009–2012 were centered in the same area as the positive anomaly measured during previous decades (1975–2008), the rate at which the more recent changes occurred is much faster. A positive gravity change of 132 μGal (after adjustment for the lava lake effect) was measured at station 205YY between March 2011 and November 2012, corresponding to a rate of increase of ~83 μGal/yr. The rate of gravity increase at the same station during 1975–2008 was just ~11 μGal/yr. Furthermore, the shorter time interval between surveys of our measurements highlights that gravity changes can fluctuate significantly over time. Gravity increased between December 2009 and June 2010 (period 1) and between March 2011 and November 2012 (periods 3 and 4) but decreased slightly between June 2010 and March 2011 (the time period that includes the March 2011 ERZ Kamoamoa fissure eruption). Although the net change over the 3 year interval is positive, gravity changes were not linear in time and reflect variations due to volcanic activity.

7.2. Accounting for the "Missing" Volume

Residual gravity changes measured between 2009 and 2012 at stations located inside Kīlauea Caldera were accompanied by surface displacements of the same area—positive changes were associated with uplift, while negative gravity changes occurred during subsidence. Our modeling results indicate, however, that even though the source of deformation and gravity change coincide—both centered at ~1.5 km beneath the northeast margin of Halema'uma'u Crater—the volume change inferred from the deformation is only 8–9% of a conservative estimate of the volume changes inferred from residual gravity variations between March 2011 and November 2012.

Our new results raise again the question of how mass can accumulate beneath the surface of Kīlauea without generating the expected uplift of the ground, as originally considered by *Johnson et al*. [2010]. Possible mechanisms include the following: (i) formation of cumulates through partial replacement of magma in the reservoir by olivine; (ii) upward migration of the magma reservoir by assimilation of host rock; (iii) filling of void space by magma, whether the space is already present (e.g., drainage of the magma reservoir during volcanic/tectonic events [see *Johnson et al*., 2010]) or forms progressively (e.g., secular extension of the summit due to rifting and "stretching" of the reservoir [*Zurek and Williams-Jones*, 2013]); (iv) bulk compression of gas-rich magma [*Johnson*, 1992; *Rivalta and Segall*, 2008] and consequent increase in density; and (v) progressive densification of the reservoir through the replacement of gas-rich magma by denser, degassed magma.

Replacement of magma (2500 kg/m^3) by denser olivine cumulates (3300 kg/m^3) is unlikely to be the main process contributing to the mass increase because ~17.0×10^6 m^3 of olivine (given the mass increase of 0.56×10^{11} kg) should have had accumulated in less than 2 years to explain the rapid residual gravity increase. Similarly, upward stoping of magma is probably not a significant source of mass increase because $>10^8$ m^3 of host rock should have been assimilated by upward migrating magma in a short time interval.

Filling of void space by magma is the preferred mechanism of previous studies, although different processes were invoked for the formation of the space [*Johnson et al*., 2010; *Zurek and Williams-Jones*, 2013]. *Johnson et al*. [2010] proposed that between 1975 and 2008, magma filled space that was created by drainage of the summit reservoir during the M_w 7.7 Kalapana earthquake in November 1975. Continuation of this process through 2012 implies a large volume of void space beneath Kīlauea Caldera or persistent formation and filling of void space at shallow levels.

Zurek and Williams-Jones [2013] proposed that rifting of the summit may also allow magma to accumulate without an increase in reservoir pressure and consequent surface uplift. In their model, an increase of 3 cm yr^{-1} (which is the rate of summit extension due to south flank motion [e.g., *Delaney et al*., 1998]) in the radius of a 1 km^3 sphere at a depth of 1 km would result in 1.45×10^5 m^3 yr^{-1} of magma to be stored without producing uplift of the surface. Such a process could explain about 16% of the measured gravity increase during 1975–2008 (the calculation in *Zurek and Williams-Jones* [2013] contains an error that led them to a

value of 59% (J. Zurek, written communication, 2013), which we correct here), demonstrating that it may be a contributor to the mass increase without causing significant vertical deformation. If we use the same approach, assuming a 1 km^3 volume reservoir at a depth of 1.5 km, magma density of 2500 kg m^{-3}, and annual volume increase of 1.45×10^5 m^3, the rate of increase in residual gravity would be 2.4 μGal yr^{-1}, resulting in 3.8 μGal of total increase between March 2011 and November 2012—only ~3% of the measured gravity increase.

Mass increase in the absence of significant inflation may also occur due to bulk compression of gas present within the reservoir as magma accumulates [*Johnson*, 1992]. Studies of geodetic measurements spanning a dike intrusion into Kīlauea's ERZ in 1997 [*Owen et al*., 2000; *Rivalta and Segall*, 2008] have shown that the volume of the intrusion was ~4 times larger than that of the deflating source reservoirs—a discrepancy that can be partially explained by compressibility of magma [*Rivalta and Segall*, 2008]. The compressibility of gas-rich magma inside the HMM reservoir during periods of surface uplift could therefore account for perhaps 32% of the mass accumulation (given that volume change alone inferred from deformation models can account for 8%) without producing the uplift that would be expected from models of pressure increase in a reservoir that is filled with incompressible magma. This process should occur during all periods of magma accumulation and might explain the moderate gravity increase between December 2009 and June 2010, which was associated with minimal uplift, and also a portion of the large positive change measured after March 2011.

Finally, ongoing summit eruptive activity may provide a means of allowing mass accumulation without significant surface uplift. The opening of the summit eruptive vent in March 2008 was associated with an order of magnitude increase in gas emissions from the summit of Kīlauea [*Elias and Sutton*, 2012]. The heightened emissions are the result of a convecting lava lake in the summit vent, which allows magma to rise to the surface, outgas, and then sink to deeper levels [*Carey et al*., 2013]. Outgassed magma could therefore progressively replace the mass of gas-rich magma that is stored within the HMM reservoir, assuming that the accumulation of outgassed magma outpaces the influx of gas-rich magma from below. If the HMM reservoir is approximated by a 1 km^3 sphere (10^9 m^3), an increase in density of 200 kg m^{-3} for the entire reservoir would produce a mass increase of 2×10^{11} kg—over 3 times the mass change needed to produce the residual gravity signal measured between March 2011 and November 2012 (~0.6×10^{11} kg). Densification of ~30% of the reservoir by 200 kg m^{-3}, or of the entire reservoir by ~65 kg m^{-3}, would therefore explain the measured residual gravity changes in the absence of surface uplift.

7.3. Gravity Changes and Eruptive Activity

The rates of the residual gravity changes over time provide further insights into the mechanism of mass variation beneath Kīlauea. The first and last time periods (December 2009 to June 2010 and June 2012 to November 2012) show the highest rates of gravity increase (68 μGal yr^{-1} and 144 μGal yr^{-1}, respectively) but are not associated with the preeruptive, coeruptive, or posteruptive phases of the March 2011 ERZ Kamoamoa fissure eruption. A slight gravity decrease was recorded during the second period (June 2010 to March 2011), which spans the Kamoamoa eruption, implying magma withdrawal from the HMM reservoir (also indicated by deflation of the reservoir). Finally, a gravity increase at lower rate (51 μGal yr^{-1}) characterizes the third period (March 2011 to June 2012), which covers the fifteen months that followed the Kamoamoa eruption. From this pattern, we conclude that the Kamoamoa eruption drew magma from the HMM reservoir, effectively "flushing" the denser, degassed magma that had been accumulating since the start of the summit eruption in 2008 and that was causing the rapid gravity increase measured during the first period. The coeruptive emptying of the reservoir was followed by rapid refilling with fresh, gas-rich magma from depth—a process that is also suggested by rapid posteruptive uplift. This resulted in a gravity increase, but at a lower rate than the first and fourth time periods (because of the lower density of the accumulating magma). During the last time period, which followed refilling of the HMM reservoir, the process of persistent degassing, convection of the lava lake, and densification of the reservoir magma resumed, accelerating the rate of gravity increase.

7.4. A Combination of Different Processes

With respect to the gravity increase measured between March 2011 and November 2012, it is likely that a combination of several of the processes discussed above is the ultimate source of the measured mass accumulation. During that time period, only ~8% of the mass increase inferred from the gravity measurements can be explained by the increase in reservoir volume inferred from modeling deformation data.

Accounting for magma compressibility, which can increase the volume of stored magma by up to 4 times without causing additional deformation [*Rivalta and Segall*, 2008], still only explains up to ~32% of the mass accumulation. Given the rapidity of the process, only minor contributions to the gravity increase could result from the formation of olivine cumulates and/or upward stoping of magma. Filling of void space with magma can easily explain the gravity increase and was the mechanism used to explain the mass accumulation measured between 1975 and 2008. This process would require, however, the presence or continued formation of void space beneath the surface. Although it may be a more significant factor over long time periods (decades), the growth of the reservoir by rifting of the summit [*Zurek and Williams-Jones*, 2013] does not significantly contribute to the mass accumulation, since the rate of gravity increase during the 20 month period far exceeds that expected from rifting. Finally, replacement of gas-rich magma by denser, outgassed magma that lost its volatiles when it reached the surface of the lava lake via convection could explain a large portion—and potentially all—of the measured gravity increase. We suspect that several processes play a role in gravity change at Kīlauea. Continued frequent (every 6–12 months) surveys of the summit gravity network in combination with deformation studies and in the context of the volcano's eruptive and intrusive activity should help to further distinguish between the relative importance of the various mechanisms.

8. Conclusions

Microgravity data collected at the summit of Kīlauea Volcano between December 2009 and November 2012 reveal significant residual gravity changes centered near Halema'uma'u Crater—a location similar to the center of the positive residual gravity anomaly measured between 1975 and 2008. Gravity changes over the 3 year period indicate a net mass accumulation at a depth of ~1.5 km, which coincides with the source of surface deformation inferred from InSAR data spanning the same time interval. This source has been previously identified as a small magma storage zone beneath the northeast margin of Halema'uma'u Crater. The rate of gravity increase, which was much higher during 2009–2012 than between 1975 and 2008, varies through time and seems to be directly correlated with the volcanic activity occurring at both the summit and the ERZ of the volcano.

InSAR data show that uplift occurred during periods of gravity increase and that subsidence characterizes a time period of slight gravity decrease—which includes the 5–9 March 2011 ERZ eruption. Despite this connection between gravity change and deformation, the volume change inferred from the modeling of the InSAR data between March 2011 and November 2012—the period of greatest gravity change—can only account for ~8% of the gravity increase (assuming that the volume increase is due to magma with a density typical of basalt).

Given the discrepancy between gravity change and surface deformation, mechanisms beyond simple filling of a magma reservoir must have occurred at Kīlauea. The replacement of gas-rich magma within the Halema'uma'u reservoir by denser, outgassed magma that had convected up to the surface within the summit eruptive vent and lost its volatiles can account for the entire residual gravity increase measured during March 2011 to December 2012. Other mechanisms, such as the compressibility of magma, the filling of void space by magma, and in minor portion the replacement of less dense material with a denser one (e.g., formation of olivine cumulate and stoping), may also contribute to the mass addition beneath the summit of Kīlauea without producing significant deformation.

Acknowledgments

Part of this research was supported by the National Aeronautics and Space Administration (NASA, NESSF11 graduate assistantship for Marco Bagnardi). The purchase of the gravimeters by the Hawaiian Volcano Observatory was made possible by the American Reinvestment and Recovery Act. The InSAR data are courtesy of the Hawai'i Supersite (CSK from ASI and TSX from DLR). We would like to thank M. Patrick and T. Orr for providing data on lava lake geometry and levels. We also thank USGS-HVO employees and volunteers that helped with the gravity surveys, including K. Anderson, S. Brantley, I. Johanson, J. Johnson, A. Learner, S. Mordensky, A. Pitty, M. Sako, and S. Wilkinson. Thanks to G. Williams-Jones, R. del Potro, and D. Dzurisin, whose comments greatly improved the manuscript. Any use of trade, firm, or product names is for descriptive purposes only and does not imply endorsement by the U.S. government.

References

Agnew, D. C. (2007), Earth tides, in *Treatise on Geophysics, Geodesy*, pp. 163–195, Elsevier, New York.

Agnew, D. C. (2010), HARDISP, in *IERS Conventions (2010)*, *IERS Tech. Note*, vol. 36, edited by G. Petit and B. Luzum, BKG (2010), pp. 99–122. [Available at http://maia.usno.navy.mil/conv2010/software.html#Ch7software.]

Baker, M. S. (2012), Investigating the dynamics of basaltic volcano magmatic systems with space geodesy, Open Access Dissertations. p. 917. [Availabe at http://scholarlyrepository.miami.edu/oa_dissertations/917.]

Baker, S., and F. Amelung (2012), Top-down inflation and deflation at the summit of Kīlauea Volcano, Hawai'i observed with InSAR, *J. Geophys. Res.*, *117*, B12406, doi:10.1029/2011JB009123.

Barnes, D. F. (1968), *Mt Hood Gravity Calibration Loop*, U.S. Geological Survey, Menlo Park, Calif.

Bartels, J. (1957), *Gezeitenkräfte,Handbuch der Physik*, Geophysik II, vol. XLVIII, Springer, Berlin.

Battaglia, M., and D. P. Hill (2009), Analytical modeling of gravity changes and crustal deformation at volcanoes: The Long Valley caldera, California, case study, *Tectonophysics*, *471*, 45–57, doi:10.1016/j.tecto.2008.09.040.

Battaglia, M., P. Segall, J. Murray, P. Cervelli, and J. Langbein (2003a), The mechanics of unrest at Long Valley caldera, California: 1. Modeling the geometry of the source using GPS, leveling and two-color EDM data, *J. Volcanol. Geotherm. Res.*, *127*, 195–217, doi:10.1016/S0377-0273(03)00170-7.

Battaglia, M., C. Roberts, and P. Segall (2003b), The mechanics of unrest at Long Valley caldera, California: 2. Constraining the nature of the source using geodetic and micro-gravity data, *J. Volcanol. Geotherm. Res.*, *127*, 219–245, doi:10.1029/2005GL024904.

Battaglia, M., J. Gottsmann, D. Carbone, and J. Fernàndez (2008), 4D volcano gravimetry, *Geophysics*, *73*(6), WA3–WA18, doi:10.1190/1.2977792.

Battaglia, M., M. P. Poland, and J. P. Kahuahikaua (2012), GTOOLS: An interactive computer program to process gravity data for high-resolution applications, Abstract GP43B-1143 presented at 2012 Fall Meeting, AGU, San Francisco, Calif., 3–7 Dec.

Berardino, P., G. Fornaro, R. Lanari, and E. Sansosti (2002), A new algorithm for surface deformation monitoring based on small baseline differential SAR interferograms, *IEEE Trans. Geosci. Remote Sens.*, *40*(11), 2375–2383, doi:10.1109/TGRS.2002.803792.

Bergstra, J., and Y. Bengio (2012), Random search for hyper-parameter optimization, *J. Mach. Learn. Res.*, *13*, 281–305.

Bos, M. S., and H.-G. Scherneck (2012), Free ocean tide loading provider, Onsala Space Observatory, Onsala, Sweden. [Availabe at http://froste.oso.chalmers.se/loading//.]

Brooks, B. A., and L. N. Frazer (2005), Importance reweighting reduces dependence on temperature in Gibbs samplers: An application to the coseismic geodetic inverse problem, *Geophys. J. Int.*, *161*, 12–20, doi:10.1111/j.1365-246X.2005.02573.x.

Carbone, D., and M. P. Poland (2012), Gravity fluctuations induced by magma convection at Kīlauea Volcano, Hawai'i, *Geology*, *40*(9), 803–806, doi:10.1130/G33060.1.

Carbone, D., G. Budetta, F. Greco, and H. Rymer (2003), Combined discrete and continuous gravity observations at Mount Etna, *J. Volcanol. Geotherm. Res.*, *123*(1), 123–135, doi:10.1016/S0377-0273(03)00032-5.

Carbone, D., M. P. Poland, M. R. Patrick, and T. R. Orr (2013), Continuous gravity measurements reveal a low-density lava lake at Kīlauea Volcano, Hawai'i, *Earth Planet. Sci. Lett.*, *376*, 178–185, doi:10.1016/j.epsl.2013.06.024.

Carey, R. J., M. Manga, W. Degruyter, H. Gonnermann, D. Swanson, B. Houghton, T. Orr, and M. Patrick (2013), Convection in a volcanic conduit recorded by bubbles, *Geology*, *41*, 395–398, doi:10.1130/G33685.1.

Cervelli, P. F., and A. Miklius (2003), The shallow magmatic system of Kīlauea Volcano, in The Pu'u 'Ō'ō-Kūpaianaha eruption of Kīlauea Volcano, Hawai'i; the first 20 years, U.S., *U.S. Geol. Surv. Prof. Pap.*, *1676*, 149–163.

Chen, C. W., and H. Zebker (2001), Two-dimensional phase unwrapping with use of statistical models for cost functions in nonlinear optimization, *J. Opt. Soc. Am. A Opt. Image Sci. Vis.*, *18*, 338–351, doi:10.1364/JOSAA.18.000338.

Chouet, B. A., P. B. Dawson, M. R. James, and S. J. Lane (2010), Seismic source mechanism of degassing bursts at Kilauea Volcano, Hawaii: Results from waveform inversion in the 10–50 s band, *J. Geophys. Res.*, *115*, B09311, doi:10.1029/2009JB006661.

Chouet, B., and P. Dawson (2011), Shallow conduit system at Kilauea Volcano, Hawaii, revealed by seismic signals associated with degassing bursts, *J. Geophys. Res.*, *116*, B12317, doi:10.1029/2011JB008677.

Davis, P. M. (1986), Surface deformation due to inflation of an arbitrarily oriented triaxial ellipsoidal cavity in an elastic half-space, with reference to Kilauea volcano, Hawaii, *J. Geophys. Res.*, *91*(B7), 7429–7438, doi:10.1029/JB091iB07p07429.

de Zeeuw-van Dalfsen, E., H. Rymer, E. Sturkell, R. Pedersen, A. Hooper, F. Sigmundsson, and B. Ofeigsson (2013), Geodetic data shed light on ongoing caldera subsidence at Askja, Iceland, *Bull. Volcanol.*, *75*, 709, doi:10.1007/s00445-013-0709-2.

Delaney, P. T., R. S. Fiske, A. Miklius, A. T. Okamura, and M. K. Sako (1990), Deep magma body beneath the summit and rift zones of Kilauea Volcano, Hawaii, *Science*, *247*(4948), 1311–1316, doi:10.1126/science.247.4948.1311.

Delaney, P. T., A. Miklius, T. Árnadóttir, A. T. Okamura, and M. K. Sako (1993), Motion of Kilauea volcano during sustained eruption from the Puu Oo and Kupaianaha vents, 1983–1991, *J. Geophys. Res.*, *98*(B10), 17,801–17,820, doi:10.1029/93JB01819.

Delaney, P. T., R. Denlinger, M. Lisowski, A. Miklius, P. Okubo, A. Okamura, and M. K. Sako (1998), Volcanics spreading at Kilauea, 1976–1996, *J. Geophys. Res.*, *103*(B8), 18,003–18,023, doi:10.1029/98JB01665.

Dvorak, J., A. Okamura, and J. H. Dieterich (1983), Analysis of surface deformation data, Kilauea Volcano, Hawaii, October 1966 to September 1970, *J. Geophys. Res.*, *88*(B11), 9295–9304, doi:10.1029/JB088iB11p.09295.

Dzurisin, D., L. A. Anderson, G. P. Eaton, R. Y. Koyanagi, P. W. Lipman, J. P. Lockwood, R. T. Okamura, G. S. Puniwai, M. K. Sako, and K. M. Yamashita (1980), Geophysical observations of Kilauea Volcano, Hawaii, 2. Constraints on the magma supply during November 1975–September 1977, *J. Volcanol. Geotherm. Res.*, *7*(3–4), 241–269, doi:10.1016/0377-0273(80)90032-3.

Eaton, J. P. (1959), A portable water-tube tiltmeter, *Bull. Seismol. Soc. Am.*, *49*(4), 301–316.

Eaton, J. P. (1962), Crustal structure and volcanism in Hawaii, in *Crust of the Pacific Basin*, *Geophys. Monogr. Ser.*, vol. 6, edited by G. A. Macdonald and H. Kuno, pp. 13–29, AGU, Washington, D. C., doi:10.1029/GM006p0013.

Efron, B., and R. J. Tibshirani (1993), *An Introduction to the Bootstrap*, *Monogr. on Stat. and Appl. Probab*, vol. 57, 436 pp., Chapman and Hall, New York.

Elias, T., and A. J. Sutton (2012), Sulfur dioxide emission rates from Kilauea Volcano, Hawaii 2007–2010, *U.S. Geol. Surv. Open File Rep.*, *2012–1107*, 25 pp.

Farr, T. G., et al. (2007), The shuttle radar topography mission, *Rev. Geophys.*, *45*, RG2004, doi:10.1029/2005RG000183.

Fattahi, H. and F. Amelung (2013), DEM error correction in InSAR time series, *IEEE Trans. Geosci. Remote Sens.*, *51*(7), doi:10.1109/TGRS.2012.2227761.

Heliker, C., and T. N. Mattox (2003), The Pu'u 'Ō'ō-Kūpaianaha eruption of Kīlauea Volcano, Hawai'i: The first 20 years, *U.S. Geol. Surv. Prof. Pap.*, *1676*.

Houghton, B. F., D. A. Swanson, R. J. Carey, J. Rausch, and A. J. Sutton (2011), Pigeonholing pyroclasts: Insights from the 19 March 2008 explosive eruption of Kīlauea volcano, *Geology*, *39*(3), 263–266, doi:10.1130/G31509.1.

Jachens, R. C., and G. P. Eaton (1980), Geophysical observations of Kilauea volcano, Hawaii, 1. Temporal gravity variations related to the 29 November, 1975, M = 7.2 earthquake and associated summit collapse, *J. Volcanol. Geotherm. Res.*, *7*(3), 225–240, doi:10.1016/0377-0273(80)90031-1.

Johnson, D. J. (1987), Elastic and inelastic magma storage at Kilauea Volcano, in *Volcanism in Hawaii*, edited by R. W. Decker, T. L. Wright, and P. H. Stauffer, *U.S. Geol. Surv. Prof. Pap. 1350*, 2, 1297–1306, U.S. Geol. Surv., Reston, Va.

Johnson, D. J. (1992), Dynamics of magma storage in the summit reservoir of Kilauea volcano, Hawaii, *J. Geophys. Res.*, *97*(B2), 1807–1820, doi:10.1029/91JB02839.

Johnson, D. J., A. A. Eggers, M. Bagnardi, M. Battaglia, M. P. Poland, and A. Miklius (2010), Shallow magma accumulation at Kīlauea Volcano, Hawai'i, revealed by microgravity surveys, *Geology*, *38*(12), 1139–1142, doi:10.1130/G31323.1.

Jonsson, S., H. Zebker, P. Segall, and F. Amelung (2002), Fault slip distribution of the 1999 Mw 7.1 Hector Mine, California earthquake, estimated from satellite radar and GPS measurements, *Bull. Seismol. Soc. Am.*, *92*, 1377–1389, doi:10.1785/0120000922.

Kauahikaua, J. (1993), Geophysical characteristics of the hydrothermal systems of Kilauea Volcano, Hawaii, *Geothermics*, *22*(4), 271–299, doi:10.1016/0375-6505(93)90004-7.

Kauahikaua, J., and A. Miklius (2003), Long-term trends in microgravity at Kīlauea's summit during the Pu'u 'Ō'ō-Kūpaianaha eruption, in *The Pu'u 'Ō'ō-Kūpaianaha Eruption of Kīlauea Volcano, Hawai'i: The First 20 Years*, *U.S. Geol. Surv. Prof. Pap.*, 1676, 165–171.

LaFehr, T. R. (1991), Standardization in gravity reduction, *Geophysics*, *56*, 1170–1178, doi:10.1190/1.1443137.

Lanari, R., O. Mora, M. Manunta, J. J. Mallorqui, P. Berardino, and E. Sansosti (2004), A small-baseline approach for investigating deformations on full-resolution differential SAR interferograms, *IEEE Trans. Geosci. Remote Sens.*, *42*, 1377–1386, doi:10.1109/TGRS.2004.828196.

Longman, I. M. (1959), Formulas for computing the tidal accelerations due to the Moon and the Sun, *J. Geophys. Res.*, *64*(12), 2351–2355, doi:10.1029/JZ064i012p02351.

Lundgren, P., et al. (2013), Evolution of dike opening during the March 2011 Kamoamoa fissure eruption, Kīlauea Volcano, Hawai`i, *J. Geophys. Res. Solid Earth*, *118*, 897–914, doi:10.1002/jgrb.50108.

McTigue, D. F. (1987), Elastic stress and deformation near a finite spherical magma body: Resolution of the point source paradox, *J. Geophys. Res.*, *92*(B12), 12,931–12,940, doi:10.1029/JB092iB12p12931.

Montgomery-Brown, E. K., D. K. Sinnett, M. Poland, P. Segall, T. Orr, H. Zebker, and A. Miklius (2010), Geodetic evidence for en echelon dike emplacement and concurrent slow-slip during the June 2007 intrusion and eruption at Kīlauea volcano, Hawaii, *J. Geophys. Res.*, *115*, B07405, doi:10.1029/2009JB006658.

Okada, Y. (1985), Surface deformation due to shear and tensile faults in a half-space, *Bull. Seismol. Soc. Am.*, *75*, 1135–1154.

Oliver, H. W., and D. F. Barnes (1968), *Mt. Hamilton Gravity Calibration Loop*, U.S. Geological Survey, Menlo Park, Calif.

Orr, T. R., W. A. Thelen, M. R. Patrick, D. A. Swanson, and D. C. Wilson (2013), Explosive eruptions triggered by rockfalls at Kīlauea volcano, Hawai'i, *Geology*, *41*, 207–210, doi:10.1130/G33564.1.

Owen, S., P. Segall, M. Lisowski, A. Miklius, M. Murray, M. Bevis, and J. Foster (2000), January 30, 1997 eruptive event on Kilauea Volcano, Hawaii, as monitored by continuous GPS, *Geophys. Res. Lett.*, *27*(17), 2757–2760, doi:10.1029/1999GL008454.

Patrick, M., and T. Orr (2011), Pattern of behavior in Kilauea's Halema'uma'u lava lake during 2011 and 1911, Abstract V34A-03 presented at 2011 Fall Meeting, AGU, San Francisco, Calif., 5–9 Dec.

Patrick, M., D. Wilson, D. Fee, T. Orr, and D. Swanson (2011), Shallow degassing events as a trigger for very-long-period seismicity at Kīlauea Volcano, Hawai'i, *Bull. Volcanol.*, *73*(9), 1179–1186, doi:10.1007/s00445-011-0475-y.

Plattner, C., F. Amelung, S. Baker, R. Govers, and M. Poland (2013), The role of viscous magma mush spreading in volcanic flank motion at Kilauea Volcano, Hawai'i, *J. Geophys. Res. Solid Earth*, *118*, 2474–2487, doi:10.1002/jgrb.50194.

Poland, M., A. Miklius, T. Orr, A. Sutton, C. Thornber, and D. Wilson (2008), New episodes of volcanism at Kilauea Volcano, Hawaii, *Eos Trans. AGU*, *89*(5), 37–38, doi:10.1029/2008EO050001.

Poland, M. P., A. J. Sutton, and T. M. Gerlach (2009), Magma degassing triggered by static decompression at Kīlauea Volcano, Hawai'i, *Geophys. Res. Lett.*, *36*, L16306, doi:10.1029/2009GL039214.

Poland, M. P., A. Miklius, A. J. Sutton, and C. R. Thornber (2012), A mantle-driven surge in magma supply to Kīlauea Volcano during 2003–2007, *Nat. Geosci.*, *5*(4), 295–300, doi:10.1038/ngeo1426.

Richter, N., M. P. Poland, and P. R. Lundgren (2013), TerraSAR-X interferometry reveals small-scale deformation associated with the summit eruption of Kīlauea Volcano, Hawai'i, *Geophys. Res. Lett.*, *40*, 1279–1283, doi:10.1002/grl.50286.

Rivalta, E., and P. Segall (2008), Magma compressibility and the missing source for some dike intrusions, *Geophys. Res. Lett.*, *35*, L04306, doi:10.1029/2007GL032521.

Rosen, P. A., S. Henley, G. Peltzer, and M. Simons (2004), Repeat orbit interferometry package released, *Eos Trans. AGU*, *85*(5), 47, doi:10.1029/2004EO050004.

Rymer, H., and G. C. Brown (1986), Gravity fields and the interpretation of volcanic structures: Geological discrimination and temporal evolution, *J. Volcanol. Geotherm. Res.*, *27*(3–4), 229–254, doi:10.1016/0377-0273(86)90015-6.

Sandwell, D., R. Mellors, X. Tong, M. Wei, and P. Wessel (2011), Open radar interferometry software for mapping surface deformation, *Eos Trans. AGU*, *92*(28), doi:10.1029/2011EO280002.

Talwani, M. (1973), Computer usage in the computation of gravity anomalies, *Methods Comput. Phys.*, *13*, 343–389.

U.S. Naval Observatory (2011), Selected astronomical constants, 2011. [Available at http://asa.usno.navy.mil/SecK/2011/Astronomical_Constants_2011.txt.]

Valiant, H. D. (1991), Gravity meter calibration at LaCoste and Romberg, *Geophysics*, *56*, 705–711.

Wilson, D., T. Elias, T. Orr, M. Patrick, J. Sutton, and D. Swanson (2008), Small explosion from new vent at Kilauea's summit, *Eos Trans. AGU*, *89*(22), 203, doi:10.1029/2008EO220003.

Wright, T. J., B. E. Parsons, and Z. Lu (2004), Toward mapping surface deformation in three dimensions using InSAR, *Geophys. Res. Lett.*, *31*, L01607, doi:10.1029/2003GL018827.

Zurek, J., and G. Williams-Jones (2013), The shallow structure of Kīlauea caldera from high-resolution Bouguer gravity and total magnetic anomaly mapping: Insights into progressive magma reservoir growth, *J. Geophys. Res. Solid Earth*, *118*, 3742–3752, doi:10.1002/jgrb.50243.1.